

Lats kinase is involved in the intestinal apical membrane integrity in the nematode *Caenorhabditis elegans*

Junsu Kang¹, Donghoon Shin², Jae-Ran Yu³ and Junho Lee^{1,*}

The roles of Lats kinases in the regulation of cell proliferation and apoptosis have been well established. Here we report new roles for Lats kinase in the integrity of the apical membrane structure. WTS-1, the *C. elegans* Lats homolog, localized primarily to the subapical region in the intestine. A loss-of-function mutation in *wts-1* resulted in an early larval arrest and defects in the structure of the intestinal lumen. An electron microscopy study of terminally arrested *wts-1* mutant animals revealed numerous microvilli-containing lumen-like structures within the intestinal cells. The *wts-1* phenotype was not caused by cell proliferation or apoptosis defects. Instead, we found that the *wts-1* mutant animals exhibited gradual mislocalization of apical actin and apical junction proteins, suggesting that *wts-1* normally suppresses the formation of extra apical membrane structures. Heat-shock-driven pulse-chase expression experiments showed that WTS-1 regulates the localization of newly synthesized apical actins. RNAi of the exocyst complex genes suppressed the mislocalization phenotype of *wts-1* mutation. Collectively, the data presented here suggest that Lats kinase plays important roles in the integrity of the apical membrane structure of intestinal cells.

KEY WORDS: *C. elegans*, Intestine, Lats kinase, Exocyst complex

INTRODUCTION

The *warts (wts)* gene, a Lats kinase homolog in *D. melanogaster*, was first identified in genetic studies. Cells with *wts* mutations exhibit extensive overgrowth due to increased cell proliferation and decreased apoptosis, suggesting that *wts* is a tumor suppressor gene (Justice et al., 1995; Xu et al., 1995). In *D. melanogaster*, *wts* acts in a pathway with *fat (ft)*, *merlin (mer)*, *expanded (ex)*, *hippo (hpo)*, *salvador (sav)*, *mats* and *yorkie (yki)*. This so-called Hpo pathway is conserved in mammals, suggesting that the functions of the pathway components might also be evolutionarily conserved. Interestingly, recent studies have revealed that the Hpo pathway may have two apparently unrelated functions. One well-known function of the Hpo pathway is to regulate cell growth and death, and maintain tissue-size homeostasis (Harvey and Tapon, 2007; Saucedo and Edgar, 2007). The loss of any of the genes in the Hpo pathway, with the exception of *yki*, leads to an increase in cell proliferation and a decrease in apoptosis due to the translocation of the *yki* protein, a transcriptional coactivator, to the nucleus (Dong et al., 2007). Consistent with the dramatic overgrowth phenotype in *D. melanogaster*, the reduction of Lats kinase gene expression through promoter hypermethylation has been implicated in several types of mammalian tumors (Jiang et al., 2006; Takahashi et al., 2005). Lats mutant flies and mice display embryonic lethality (McPherson et al., 2004; St John et al., 1999; Xu et al., 1995), demonstrating that Lats kinase plays an essential role in development.

A second, although not well characterized, function of the Hpo pathway is its involvement in cell polarity. For example, in *D. melanogaster*, *wts* is involved in cell-shape maintenance, dendritic maintenance and oocyte axis specification (Emoto et al., 2006;

Meignin et al., 2007; Polesello and Tapon, 2007). During oogenesis in the fly, the Hpo pathway regulates differentiation of the polar follicle cell (PFC). Mutations in the core Hpo pathway genes in the PFC lead to a misoriented mitotic spindle, a multilayered epithelium and abnormal cell polarity, consistent with the Hpo pathway being involved in the regulation of cellular polarity. However, it is not yet known whether the Hpo pathway participates in establishing or maintaining the cellular polarity of the PFC, although in fission yeast *orb6*, a Lats kinase homolog, is known to be involved in the maintenance of cell polarity (Verde et al., 1998). *cbk1*, the budding yeast homolog of Lats kinase, regulates polarized cell growth (Bidlingmaier et al., 2001). Several reports also suggest that Lats kinase is involved in information processing, from cell contact to cell proliferation (Zhao et al., 2007). In addition, the Hpo pathway has been implicated in the regulation of intracellular trafficking because the endocytic trafficking of the Notch receptor is affected in the Hpo pathway mutant PFC (Yu et al., 2008). All of these data suggest the possibility of an evolutionarily conserved role for Lats kinase in the regulation of intracellular trafficking in order to control cellular polarity. Because *C. elegans*, a soil nematode, contains a single homolog of Lats kinase, we decided to examine its possible roles in development in the hope of elucidating evolutionarily conserved Lats kinase mechanisms of action.

C. elegans is a useful genetic model organism, the development of which has been extensively characterized. Epithelial tissues of *C. elegans*, the intestine, the pharynx and the hypodermis, are separated by the apical surface, bordered by the *C. elegans* apical junction (Ce_AJ), and have distinct basolateral surfaces that contact both adjacent cells and the underlying basement membranes. The proteins required for cell polarity are well conserved in *C. elegans* and their localizations are similar to polarity proteins in other species (Cox and Hardin, 2004). In particular, the intestine of *C. elegans* is a highly polarized tissue, the apical-basal polarity of which is easily observed in a single microscopic focal plane, making it a useful system for the study of cellular integrity (Leung et al., 1999). In this study, we first analyzed WTS-1, the *C. elegans* Lats homolog, to show that it localizes to the membrane in a variety of epithelial tissues, especially at the subapical membrane in the intestine. We

¹Research Center for Functional Cellulomics, Institute of Molecular Biology and Genetics, School of Biological Sciences, Seoul National University, Seoul 151-747, Korea. ²College of Medicine, Seoul National University, Seoul 110-799, Korea.

³Department of Environmental and Tropical Medicine, School of Medicine, Kon-Kuk University, Seoul 143-701, Korea.

*Author for correspondence (e-mail: elegans@snu.ac.kr)

then show that WTS-1 plays an important role in the cellular integrity of intestinal cells. Additionally, we demonstrate that a mutation in *wts-1* results in larval arrest due to defects in the regulation of protein localization, as revealed by electron microscopy and molecular genetic tools. Our genetic and molecular data suggest that WTS-1 is involved in the maintenance of cellular integrity of the intestine.

MATERIALS AND METHODS

Strains

The Bristol strain, N2, was used as the wild-type (WT) and handled using standard protocols. The following N2-derivative strains were used: *wts-1(ok753)*, *dpy-5(e61)* *daf-16(m26)* *unc-75(e950)*, *rrf-3(pk1426)* and *ced-2(e1752)*. The hT2[qIS48] balancer chromosome, which has a pharyngeal GFP signal, was used as a dominant chromosome I balancer. The GFP signal was used as a marker for identifying control heterozygous animals with a *wts-1* mutation.

Molecular biology

The full-length *wts-1* genomic DNA, plus 2.7 kb of the promoter sequence, was cloned into the GFP-containing pPD 95.75 vector. For *dlg-1*, the full-length genomic DNA was cloned into pPD 95.77 under the control of the *act-5* promoter (*Pact-5*). For *hmp-1*, the nearly full-length genomic DNA with approximately 3 kb of the 5' sequence was cloned into pPD 95.75. For *act-5*, 2 kb of the promoter sequence of *act-5* was cloned into pPD 117.01 and the full-length *act-5* genomic DNA was inserted after the C-terminus of GFP. For *vha-6*, the full-length cDNA of *vha-6* was cloned into pPD 114.108 under the control of the *opt-2* promoter. For *opt-2*, pKN111 was used (a gift from K. Nehrke) (Nehrke, 2003). For *pbo-4* and *inx-3*, the full-length genomic DNA of *pbo-4* or *inx-3* was cloned into pPD 114.108 under the control of the *opt-2* promoter. For the *wts-1* RNAi vector, the *wts-1* cDNA (bases 350-1550) was cloned into the L4440 vector.

Transgenic lines

To make *wts-1::gfp* transgenic worms, we injected a *wts-1::gfp* construct into the WT worms at 100 µg/ml with the pRF4 selection marker. At least three independent transgenic worm lines were obtained. For other transgenic worms, unless otherwise indicated, all plasmids were injected into N2 or VC590 worms (*wts-1* heterozygotes) at 100 µg/ml, with either the pRF4 selection marker or the *sur-5::gfp* fluorescence marker.

Microscopy

Time-lapse images (Fig. 1D), immunostained images (Fig. 1E,F), 3D images (Fig. 2D,E) and fluorescence images (Fig. 3A) were acquired using the DeltaVision system (Applied Precision) equipped with an inverted microscope (IX71, Olympus), a 100× 1.3 NA oil lens (Olympus), a CCD camera (CoolSNAP HQ) and softWoRx software (Applied Precision). These images were deconvolved using SoftWorx. All other images were acquired with a microscope (Axioplan 2, Carl Zeiss), a 100× 1.3 NA oil lens (Carl Zeiss), a CCD camera (AxioCam HRC) and AxioVision 4 software (Carl Zeiss).

Optical section images (Fig. 2D,E) were taken using the DeltaVision system and deconvolved using the softWoRx program. Images were taken as 50 sections along the *z*-axis at 0.2 µm intervals. Images were merged into a single projection image and reconstructed into 3D images using the Imaris projection (Bitplane).

WTS-1::GFP expression analysis

wts-1::gfp transgenic embryos and worms were mounted on a 5% agar pad and observed under a microscope. Four-dimensional time-lapse video microscopy was performed using the DeltaVision system. *wts-1::gfp* gravid adults were cut and embryos were harvested, mounted on the 5% agar pad and sealed with Vaseline. Time-lapse images were taken every 5 minutes for 2 hours at room temperature.

Antibodies and immunostaining

Antibody staining of embryos was performed using the freeze-cracking method, as previously described (Bossinger et al., 2004). Primary and secondary antibodies were used at the following concentrations: PAR-3,

1:50 (DSHB, P4A1); PKC-3, 1:1000 (a gift from K. Kemphues, Cornell University, Ithaca, NY, USA); anti-mouse Alexa 568, 1:1000 (Molecular Probes); and anti-rat TRITC, 1:500.

Intestinal integrity test

Gravid adults of heterozygous *wts-1* mutant animals that expressed *gfp::act-5*, *Pact-5-dlg-1::gfp*, *hmp-1::gfp*, *Popt-2-vha-6::gfp*, *Popt-2-pbo-4::gfp* or *Popt-2-inx-3::gfp* were transferred to new NGM plates and embryos were collected for 12 hours. The next day, the gravid adults were removed, and control worms (heterozygotes), which express pharyngeal GFP, and mutant worms (homozygotes), which do not express pharyngeal GFP, were transferred to new *E. coli*-free NGM medium. After 1 or 2 days, control and mutant worms were analyzed.

Heat-shock-based GFP::ACT-5 pulse-chase experiment

L1 worms of control (*wts-1* heterozygous) and 1-day-, 2-day- or 3-day-old *wts-1* mutant worms that expressed GFP::ACT-5 under the control of the *hsp-16.41* promoter were placed at 33°C for 20 minutes and then allowed to recover at 20°C. GFP::ACT-5 expression was observed at 0 minutes or 60 minutes, or 2 days later.

RNAi screening

RNAi by feeding was performed using standard methods. To identify the suppressors of *wts-1*, we focused on genes that were known or predicted to function in protein trafficking. *E. coli* strains containing each RNAi clone were obtained from the RNAi library (J. Ahringer, Wellcome Trust/Cancer Research UK Gurdon Institute, Cambridge, UK). For the exocyst complex gene RNAi, *sec-3*, *sec-8*, *sec-10*, *sec-15* and *exoc-7* clones from the RNAi library were used. For the *sec-6* and *exoc-8* RNAi, full-length cDNAs were cloned into L4440. For the *sec-5* RNAi, genomic DNA of *sec-5* was digested with *Bgl*II and *Xba*I (between the eighth and ninth exons) and cloned into L4440. The genotype of the worms used in this assay was *wts-1(ok753)/hT2*; *Ex[gfp::act-5, pRF4]*. Chromosome hT2 is a genetic balancer and is recognized easily by pharyngeal GFP. L3 and L4 transgenic worms were grown to the adult stage on the RNAi medium. When they had reached the adult stage, they were transferred to new RNAi medium and allowed to lay eggs for 12 to 16 hours; then the adults were removed. After 3 days at 20°C, mutant worms that showed no pharyngeal GFP signal were examined for GFP::ACT-5 localization.

Electron microscopy

L1 larvae of N2 and *ok753* animals were harvested, as described previously (MacQueen et al., 2005). To obtain the *ok753* homozygous animals, we used *wts-1(ok753)/dpy-5(e61)* *daf-16(m26)* *unc-75(e950)* worms. Electron microscopy was performed as previously described (Ko et al., 2007).

Cell numbers

To count the number of intestinal cells, we performed DAPI staining. Images were taken using a multi-photon laser scanning microscope (Zeiss LSM 510, Carl Zeiss). Because intestinal cells divide during development without cytokinesis, they contain endoduplicated nuclei (Hedgecock and White, 1985). Both the L1-arrested control and terminally L1-arrested *wts-1(ok753)* mutant animals had endoduplicated nuclei, which we counted as one intestinal cell. We determined the number of intestinal cells in the L1-arrested N2 and 3 day *wts-1(ok753)* mutant animals.

To count the number of cells undergoing mitosis in the gonads, we used the *wts-1(ok753)*; *Ex[Popt-2::wts-1, sur-5::gfp]* and N2 strains. L4 worms were transferred to new medium and were cut the following day. The gonads were fixed with methanol and then stained with DAPI. We counted mitotic cells that had condensed shapes in each gonad under a microscope. To count the number of progeny, we used the N2 and *wts-1(ok753)*; *Ex[Popt-2::wts-1, sur-5::gfp]* strains. A single L4 animal was transferred to NGM medium and every 12 hours was retransferred to new medium. The total number of embryos produced was counted.

Cell corpse measurement

To count cell corpse numbers, we used the *ced-2(e1752)* and *wts-1(ok753)*; *ced-2(e1752)*; *Ex[wts-1, sur-5::gfp]* strains. Cell corpses in the head of young L1 were counted. To count the number of cell corpses in the gonad,

we used the N2 and *wts-1(ok753)*; Ex[P*wts-1::wts-1, sur-5::gfp*] animals. Cell corpses were counted in adult worms (24-36 hours after the L4/adult molt).

Acridine Orange and TRITC-dextran treatment

The endocytosis assay was performed as previously described (Grant et al., 2001).

GFP-*E. coli* feeding assay

Gravid adults were transferred to new NGM plates and embryos were obtained for 2-3 hours. The GFP signals in the intestine of N2, *wts-1(ok753)*; Ex[P*opt-2::wts-1, pRF4*] and *wts-1(ok753)* worms were checked for remaining GFP fluorescence either 12 hours or 3 days after hatching.

Defecation assay

Defecation assays were performed as previously described with some modifications (Liu and Thomas, 1994). We used L1 animals ~5-7 hours after hatching. The defecation behavior was observed for 10 minutes.

RESULTS

WTS-1, the putative homolog of Lats kinase, localizes to the subapical region of epithelial cells

By searching the *C. elegans* genome database, we have identified a single gene that encodes a Lats kinase, *wts-1*. WTS-1 has features of the NDR kinase family, including long N-terminal sequences (Fig. 1A; see Fig. S1 in the supplementary material) (Hergovich et al., 2006). As an initial step towards elucidating the function of WTS-1, we examined its expression and subcellular localization. WTS-1::GFP was widely expressed in epithelial and muscular tissues in all developmental stages examined, from embryo to adult. WTS-1::GFP was present in the cytoplasm and, interestingly, also localized to the membrane in epithelial tissues (the vulva, the spermatheca, the intestine, the hypodermis, the excretory canal and the pharynx; Fig. 1B,C; data not shown). Although WTS-1::GFP did not localize to the membrane in early embryos, it localized to the membrane in late embryos. To determine the precise stage in development when WTS-1::GFP moved to the membrane, we monitored the changes in WTS-1::GFP localization during embryogenesis using time-lapse microscopy. In the pharynx, WTS-1::GFP localized to the membrane during the epithelization stage (Fig. 1D) (Portereiko and Mango, 2001). In the intestine, WTS-1::GFP showed a similar pattern to that of HMR-1 (Fig. 1D) (Leung et al., 1999).

To determine the exact subcellular localization of WTS-1::GFP in the intestine, we compared WTS-1::GFP localization with the localization of PAR-3, a protein that localizes to the apical part of the lateral membrane, and PKC-3, a protein that localizes to the apical membrane (Totong et al., 2007). We found that WTS-1::GFP broadly colocalized with PAR-3 (Fig. 1E) and PKC-3 (Fig. 1F). WTS-1::GFP additionally showed localization lateral to PKC-3 and localization apical to PAR-3 (Fig. 1E,F), suggesting that WTS-1::GFP localizes to the subapical regions in the intestine.

wts-1 mutant animals have a larval arrest phenotype and show defects in intestinal structure

To identify the physiological consequences of losing *wts-1* function, we analyzed the phenotype of *wts-1* mutant animals. The *wts-1(ok753)* mutation is a deletion that deletes the kinase domain (Fig. 2A), which should be a loss-of-function mutation, if not a null mutation. The major mutant phenotype was an early larval arrest that was confirmed by *wts-1* RNAi experiments (see Table S1 in the supplementary material). Rescue experiments with WTS-1::GFP and other WTS-1 constructs confirmed that the observed phenotype

was solely due to the mutation of *wts-1*. Interestingly, the intestine-specific expression of *wts-1* using an expression construct driven by the *opt-2* promoter (Nehrke, 2003) was sufficient to rescue the defects (Fig. 2H), suggesting that the zygotic expression of *wts-1* in the intestine is sufficient for survival. The percentage of worms rescued with the *wts-1* and *opt-2* promoters was 88% ($n=97$) and 74% ($n=126$), respectively. In an attempt to identify specific causes of the intestinal defects, we first performed a GFP-*E. coli* feeding assay. Whereas the wild-type (WT) N2 animals, intestine-specific *wts-1*-rescued worms and the *wts-1* mutant animals were able to absorb GFP-*E. coli* 12 hours after hatching, with almost no GFP was detected in the intestine ($n=138$, 36 and 46 for WT, rescue line and mutant, respectively), 3-day-old *wts-1* mutant animals accumulated GFP-*E. coli* in their intestine ($n=104$) (see Fig. S2 in the supplementary material). To examine whether defective defecation caused the accumulation of bacteria in the mutant intestine, we examined defecation rates of the control and mutant animals at their L1 stages ($n=10$ for each strain). *wts-1* mutant worms showed partially defective defecation, suggesting that the main reason for bacterial accumulation in the *wts-1* mutant animals is a defect in defecation (see Fig. S2 in the supplementary material). Additionally, the fact that intestinal WTS-1 expression alone rescued the mutant phenotype suggests that the loss of *wts-1* function in the intestine, but not in the pharynx, rectum or other organs, was necessary for the phenotype (see Fig. S2 in the supplementary material). Because the intestine is important for defecation (Branicky and Hekimi, 2006), it is possible that the intestine is defective in its role in defecation in *wts-1* mutant animals.

Next, using a differential interference contrast microscope, we observed that many terminally arrested *wts-1(ok753)* animals contained extra structures in addition to the normal-looking intestinal lumen (Fig. 2B,C). To analyze the intestinal defects more closely, we generated three-dimensional optical section images of GFP::ACT-5 in the WT and *wts-1* mutant animals. The *wts-1* mutant animals showed basolateral and vesicle-like accumulations of GFP::ACT-5, in addition to the normal-looking intestinal lumen (Fig. 2D,E). To further characterize these structures, we obtained transmission electron microscopy (TEM) images of terminally arrested mutant animals. Whereas WT worms had a single normal lumen, *wts-1* mutant worms had two or more lumen-like structures (Fig. 2F,G; see Fig. S3 in the supplementary material). Interestingly, these extra lumen-like structures contained normal-looking microvilli on the apical side. Among several lumen-like structures in the *wts-1* mutant worms, only one structure had a thicker apical membrane, suggesting that the mutant worm had only one main lumen surrounding the thicker apical membrane and that the other structures might not originate from the main lumen (see Fig. S3 in the supplementary material). Consistent with our interpretation, GFP-*E. coli* were never found in the lumen-like structures in the *E. coli* feeding assay described above. Although mutant animals had intact Ce_AJs within their intestines, the number of Ce_AJs was abnormal (Fig. 2F,G; see Fig. S3 in the supplementary material). We did not observe any extra intestinal cells in the *wts-1* mutant animals (see below; Fig. 2I), suggesting that the abnormal lumen structures were not due to the overproliferation of intestinal cells.

WTS-1 might not be involved in the control of cell proliferation and cell death in *C. elegans*

In flies and mammals, Lats kinases regulate tissue size by controlling cell proliferation and apoptosis through their involvement in Hpo signaling. Therefore, we examined whether *wts-1* is involved in cell proliferation and apoptosis in *C. elegans*.

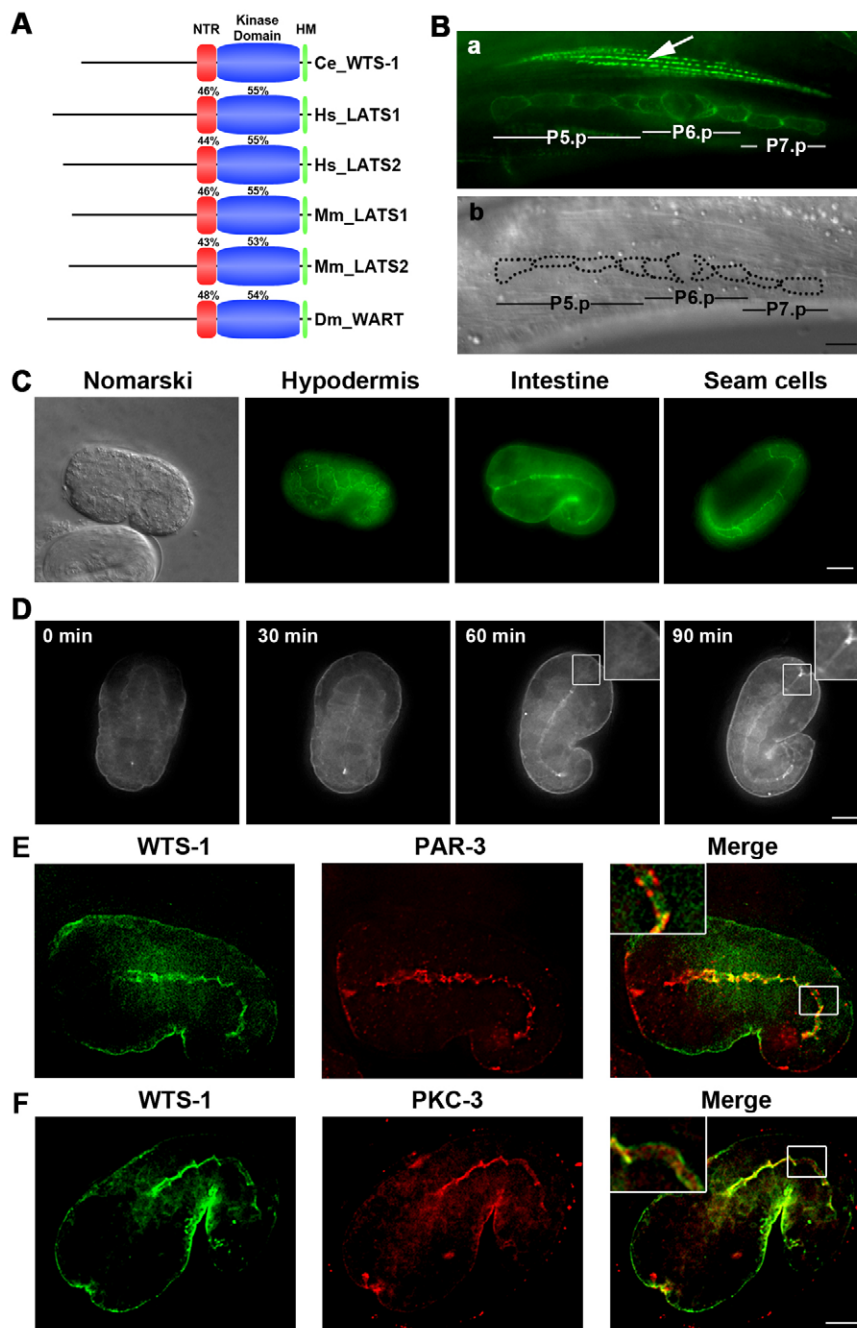


Fig. 1. WTS-1, the putative *C. elegans* homolog of mammalian Lats kinase, localizes to the subapical region in the intestine. (A) Domain structure of WTS-1 homologs. NTR, N-terminal regulatory domain; HM, hydrophobic motif. Numbers indicate the percentage amino acid identity with respect to *wts-1*. (B) Ventral view showing *wts-1* expression in the vulval precursor cells (VPCs). (a) Fluorescence image; (b) matching Nomarski image, dotted lines indicate VPC outlines. VPC lineages are shown. Arrow indicates WTS-1::GFP expression in the body wall muscle. (C) Embryonic *wts-1* expression. Lateral views showing WTS-1::GFP localization in the indicated tissues. (D) Time-lapse images of WTS-1::GFP in the intestine during embryogenesis. Ventral enclosure begins at time 0. (E, F) Subcellular localization of WTS-1::GFP in the intestine. *wts-1::gfp* transgenic embryos were immunostained with PAR-3 (E) and PKC-3 (F) antibodies (red), with WTS-1::GFP in green. Insets in D-F are magnified images. Scale bars: 10 μ m.

First, we determined the number of intestinal cells in N2 control and 3-day-old *wts-1* mutant animals. Both animals had 20 or 21 intestinal cells ($n=9$ and 6, s.d.=0.3 and 0 for N2 and mutant animals, respectively; Fig. 2I), suggesting that the *wts-1* mutation does not cause overproliferation of intestinal cells. Next, we determined the number of progeny from the *wts-1* mutant hermaphrodites. If the *wts-1* mutation caused overproliferation of germ cells, including sperm, the mutant animals might produce more progeny than WT hermaphrodites. *C. elegans* hermaphrodites produce only a limited number of progeny (~300) because they produce a limited number of sperm during their lifetime. We examined the *wts-1* mutant worms in which WTS-1::GFP was expressed under the intestine-specific *opt-2* promoter, so that other tissues carried the *wts-1* homozygous mutation. N2 WT worms were used as positive controls. The average number of progeny from both strains was not

significantly different: 223 for the control and 163 for the intestine-specific rescue line. This suggests that the *wts-1* mutation does not cause over-proliferation of male germ cells ($n=5$ for both strains; s.d.=53 and 45 for the intestine-specific rescue line and the control, respectively) (Fig. 2J). Next, we compared the numbers of germ cells undergoing mitosis in the gonad of the control and intestine-specific rescue worms (Fig. 2K). The control gonads contained an average of 2.13 mitotic cells per gonad arm ($n=67$, s.d.=1.09) and the gonad of intestine-specific rescue worms contained an average of 2.02 mitotic cells per gonad arm ($n=72$, s.d.=1.3). To examine whether *wts-1* affects apoptosis, we made a *wts-1*; *ced-2* double mutant line and counted the number of persistent cell corpses in the heads of young L1 larvae (Fig. 2L). The average number of cell corpses in *ced-2(e1752)* single mutant animals was 16.03 and number of cell corpses in the *wts-1(ok753)*; *ced-2(e1752)* double

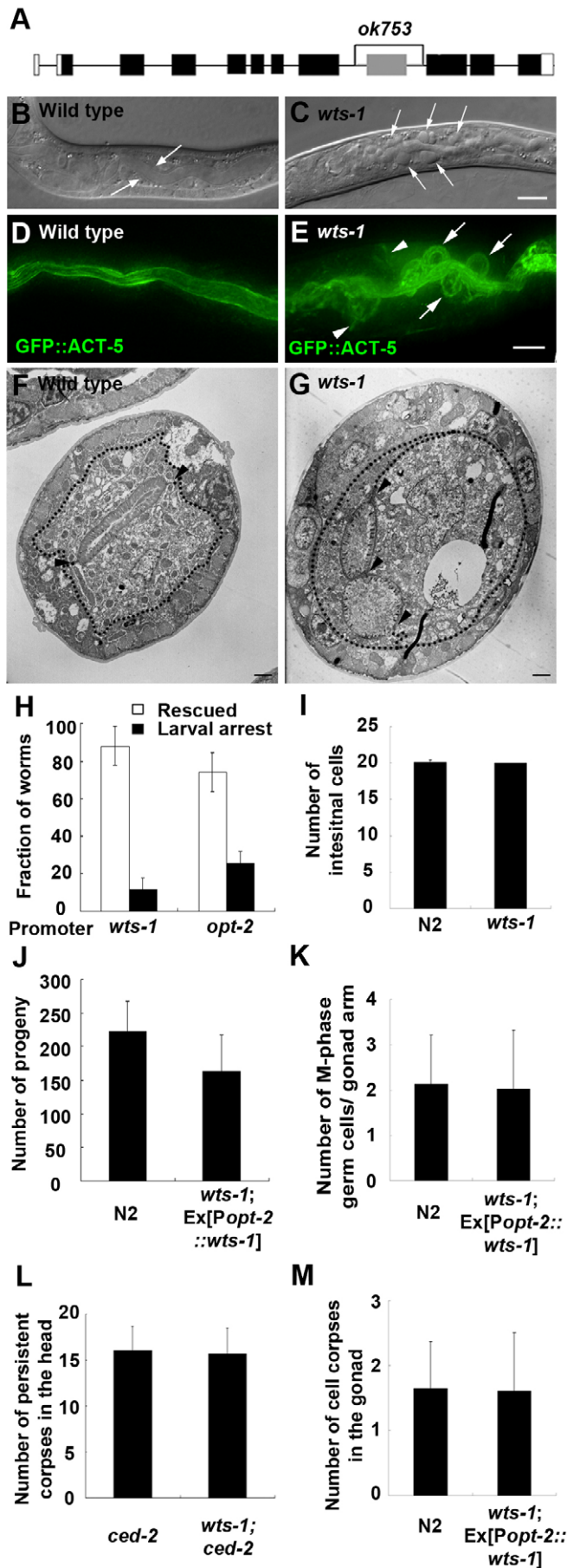


Fig. 2. A loss-of-function mutation in *wts-1* causes a larval arrest phenotype and intestinal defects. (A) Structure of *wts-1* gene. Exons are shown as boxes with connecting lines depicting introns. White boxes denote untranslated regions. The deleted region in the *wts-1(ok753)* mutation is indicated and was confirmed by RT-PCR. The ninth exon encoding the kinase domain (gray) is deleted.

(B-G) Intestinal defects caused by the *wts-1(ok753)* mutation. (B,C) Nomarski images of WT (B) and *wts-1(ok753)* mutant (C) animals. Arrows in B indicate the normal intestinal lumen. Vesicle-like structures (C, arrow) are evident next to the intestinal lumen of the *wts-1(ok753)* mutant animal. (D,E) Three-dimensional optical section images of WT (D) and *wts-1(ok753)* mutant (E) animals expressing GFP::ACT-5. Arrows indicate GFP::ACT-5-containing structures and arrowheads indicate laterally localized GFP::ACT-5 (E). (F,G) TEM images of WT (F) and *wts-1(ok753)* mutant (G) animals. The WT animal had a single normal lumen (F), but the *wts-1(ok753)* mutant animal had two lumen-like structures (G). Arrowheads indicate apical junctions, dotted lines indicate the boundaries of intestinal cells. (H) Quantification of results of the rescue experiment with WTS-1 expression constructs under the control of either the *wts-1* promoter or the intestinal *opt-2* promoter. (I-M) The *wts-1* mutation does not cause overproliferation or reduced apoptosis. (I) Number of intestinal cells in N2 and *wts-1* mutant animals. (J) Number of progeny embryos in N2 and *wts-1* worms rescued with the WTS-1::GFP expression construct under the control of the intestinal promoter (*opt-2*). (K) Number of cells undergoing mitosis in the gonad arms of N2 and *wts-1* mutant young adults rescued with intestinal WTS-1 expression. (L) Number of persistent cell corpses in the heads of *ced-2* and *wts-1; ced-2* L1 mutant animals. (M) Number of cell corpses in the gonads of N2 and *wts-1* worms rescued with the WTS-1::GFP construct under the control of the intestinal promoter (*opt-2*). Scale bars: 10 μ m in C,E; 1 μ m in F,G.

mutant animals was 15.63 ($n=24$ and 22, s.d.=2.69 and 2.92 for *ced-2* and *wts-1; ced-2*, respectively). In addition, we counted the number of cell corpses in the gonads of N2 WT and the intestine-specific rescue line animals. Both had similar numbers of cell corpses in the gonads of young adults (Fig. 2M). The average number of cell corpses in N2 animals was 1.64 and the number of cell corpses in the intestine-specific rescue line was 1.61 ($n=28$ and 23, s.d.=0.73 and 0.89 for N2 and intestine-specific rescue line, respectively). These results suggest that the *wts-1* mutation might not cause either overproliferation or decreased apoptosis in *C. elegans*.

The *wts-1* mutation causes the mislocalization of apical actin and apical junction proteins to the extra apical membrane structure

We next examined the possibility that the intestinal defect in the *wts-1* mutant animals is caused by the disruption of membrane integrity. To do this, we examined the localization of several intestinal apical proteins: ACT-5 as an intestinal actin marker; HMP-1 as a cadherin-catenin complex (CCC) marker; and DLG-1 as a DLG-1-AJM-1 complex marker. (Bossinger et al., 2001; Costa et al., 1998; MacQueen et al., 2005). The CCC proteins are localized more apically than the DLG-1-AJM-1 complex proteins. We used *wts-1* heterozygotes that contained the hT2 balancing chromosome with an integrated pharyngeal GFP expression cassette as controls; because hT2 can be recognized with pharyngeal GFP, control worms would have pharyngeal GFP expression and *wts-1* mutant worms would not. Over the course of 3 days, we examined *wts-1* mutant animals that were arrested at the L1 stage due to the mutation and,

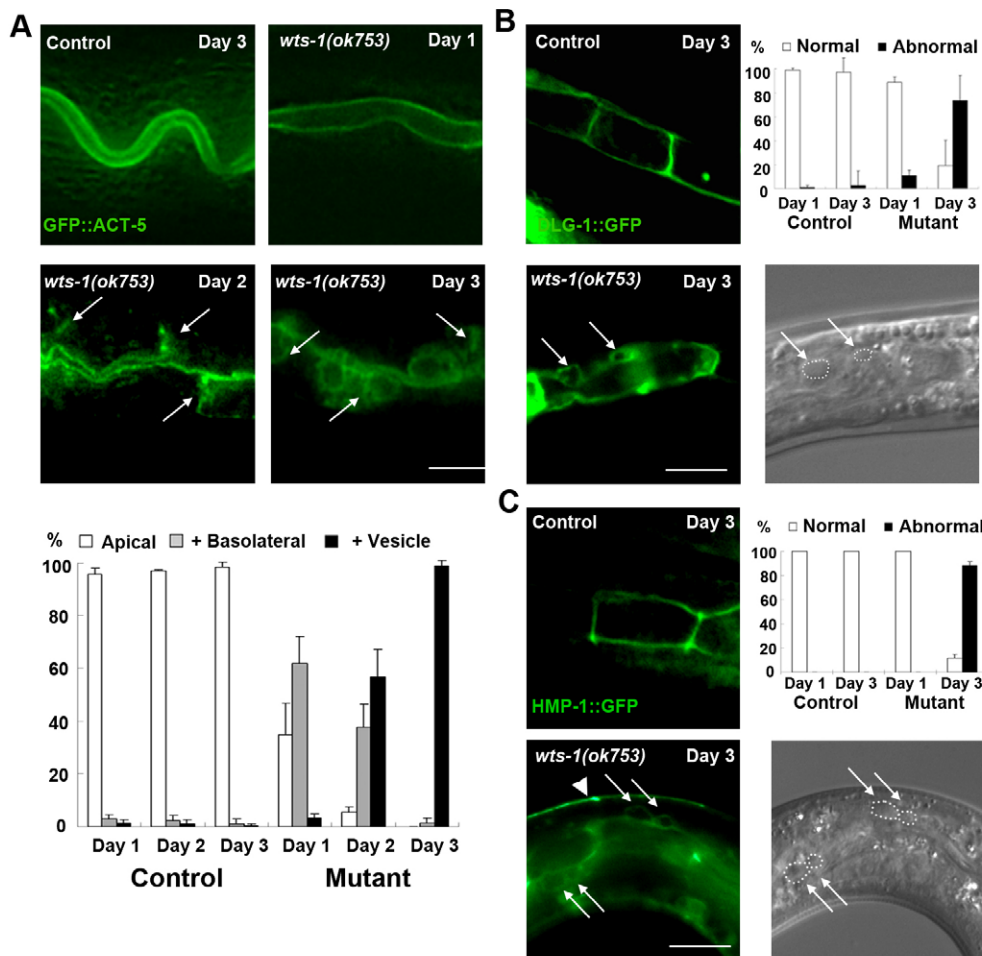


Fig. 3. The *wts-1(ok753)* mutation causes the gradual abnormal localization of intestinal actin and apical junctional proteins.

(A) Expression patterns of GFP::ACT-5 in control (heterozygote of *wts-1*) and *wts-1(ok753)* mutant worms. The severity of the ectopic localization phenotype increased in a time-dependent manner in *wts-1* mutant animals. Arrows indicate basolaterally localized GFP::ACT-5. The bottom graph shows quantification of the results. '+ Basolateral' indicates animals that showed apical and basolateral localization of the protein; '+ Vesicle' indicates animals that had protein localized in the vesicle-like structures, in addition to the apical and basolateral sides. (B,C) DLG-1::GFP (B) and HMP-1::GFP (C) localization in control (heterozygous for *wts-1*) and *wts-1(ok753)* mutant worms. The graphs show quantification of the results. 'Normal' indicates animals that show the rectangular form; 'Abnormal' indicates animals that show the additional localization to basolateral or vesicle-like structures. Arrows indicate ectopic vesicle-like structures next to the intestinal lumen. Arrowhead in C indicates hypodermal expression of HMP-1::GFP, which is occasionally observed in the same focal plane. Scale bars: 10 μ m.

as controls, heterozygous animals that were arrested at the L1 stage by starvation. *wts-1* heterozygous L1 animals had a constitutive apical localization of GFP::ACT-5, even 3 days after they were placed on the *E. coli*-free medium (Fig. 3A; see Table S2 in the supplementary material). By contrast, the GFP::ACT-5 localization was gradually altered in the *wts-1(ok753)* homozygous animals. Localization to the apical membrane remained unchanged, but GFP::ACT-5 gradually spread to the basolateral sides or ectopic apical surfaces of the basolateral sides and then to the intracellular vesicle-like structures (Fig. 3A; see Table S2 in the supplementary material). These data indicate that in the *wts-1* mutant animals, the GFP::ACT-5 localization is limited to the apical membrane at the beginning of the larval stage, but eventually becomes dispersed to the basolateral sides and then to the vesicle-like structures. The other markers, HMP-1::GFP and DLG-1::GFP, showed similar localization patterns to that of GFP::ACT-5 (Fig. 3B,C; see Table S2 in the supplementary material).

We then examined the localization patterns of more marker proteins in *wts-1* mutant animals in order to determine whether the *wts-1* mutant phenotype affects protein localization in general. GFP reporters of VHA-6 and OPT-2, two apical proteins (Nehrke, 2003; Oka et al., 2001), showed only apical localization in the intestine in nearly all of the day 1 and day 3 controls and *wts-1* mutant animals (Fig. 4A-H; see Table S2 in the supplementary material). As basolateral markers, we examined the localization of PBO-4::GFP and INX-3::GFP (Pfeiffer et al., 2008; Starich et al., 2003). Because PBO-4::GFP and INX-3::GFP transgenic *wts-*

1 mutant animals had a more severe larval lethal phenotype for unknown reasons, we examined the *wts-1* arrested animals that expressed PBO-4::GFP and INX-3::GFP as genetic mosaics on day 3 after egg laying. The localization patterns of PBO-4::GFP and INX-3::GFP in *wts-1* mutant animals did not differ from those in WT animals (Fig. 4I-L; see Table S2 in the supplementary material), suggesting that the *wts-1* mutation does not affect the localization of basolateral proteins. Therefore, we conclude that *wts-1* is involved in the regulation of the localization of a subset of apical and apical junction proteins without affecting global protein localizations. Collectively, these data suggest that *wts-1* normally suppresses the formation of extra apical membrane structure by inhibiting the mislocalization of intestinal apical actin, the CCC and the DLG-1-AJM-1 complex proteins in the intestine.

The newly synthesized GFP::ACT-5 is mislocalized to the ectopic luminal domain and the exocyst complex is required for the mislocalization

The observation that GFP::ACT-5 localization is gradually dispersed from the apical membrane to the basolateral sides and then to vesicle-like structures in the *wts-1* mutant animals raised the possibility that the localization defect is caused by the abnormal cellular trafficking of proteins involved in the local assembly and disassembly of apical actin. To investigate this possibility, we first examined the apical endocytosis markers in *wts-1* mutant animals. Endocytosed vesicles from the apical membrane of *C. elegans* can

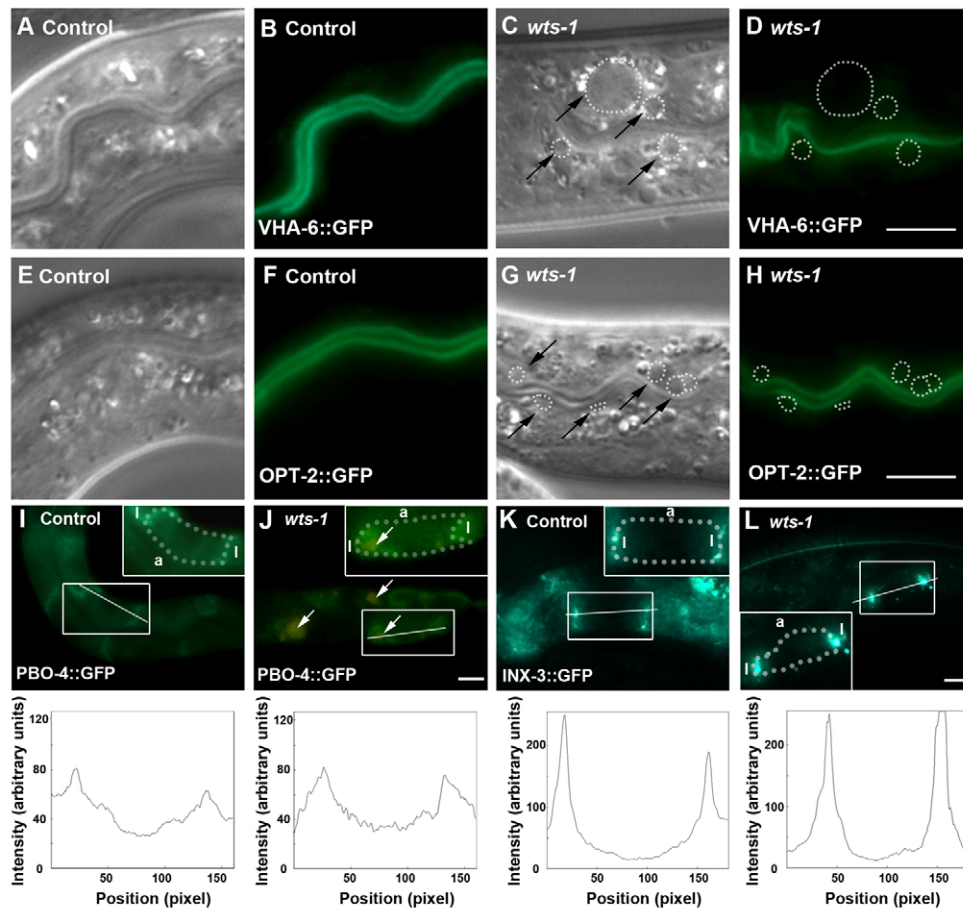


Fig. 4. Not all apical and basolateral proteins are mislocalized in the *wts-1(ok753)* mutant animals. (A-D) Expression pattern of VHA-6::GFP in control (A,B) and *wts-1(ok753)* mutant (C,D) worms. **(E-H)** Expression pattern of OPT-2::GFP in control (E,F) and *wts-1(ok753)* mutant (G,H) worms. Arrows indicate ectopic vesicle-like structures (white dotted circles) next to the intestinal lumen (C,G). **(I-L)** Expression patterns of PBO-4::GFP (I,J) and INX-3::GFP (K,L) in control (I,K) and *wts-1(ok753)* mutant (J,L) worms. Insets in I-L are magnified images; a, apical parts and l, lateral parts of intestinal cells, respectively; dotted line marks cell outline. Arrows in J indicate autofluorescence signals. The graphs below show fluorescence quantification in which PBO-4::GFP or INX-3::GFP fluorescence intensity as a function of position was graphed using AxioVision software along the lines shown in the figures I-L. Scale bars: 10 μ m.

be detected with several endocytic tracers [e.g. Acridine Orange (AO) and TRITC-dextran], which are taken up by the intestinal lumen and accumulate in the gut endocytic vesicles (Grant et al., 2001). We fed AO or TRITC-dextran to *wts-1* mutant animals and found that the tracers localized to the intestine, suggesting that endocytosis is functional in the mutant animals. However, AO and TRITC-dextran did not localize within the vesicle-like structures (Fig. 5A,B), suggesting that the ACT-5-containing vesicles observed in the mutant animals are not the terminal endosomes ($n=14$ and 20 for AO and TRITC-dextran experiments, respectively).

We then examined whether the GFP::ACT-5 localization defect was caused by the mislocalization of newly synthesized GFP::ACT-5 or the mislocalization of apically localized GFP::ACT-5. To do this, we designed a heat-shock-based GFP::ACT-5 pulse-chase experiment. We generated transgenic *wts-1* heterozygote worms that have a *gfp::act-5* transgene under the control of a heat shock promoter. We delivered a pulse of heat shock to induce the expression of newly synthesized GFP::ACT-5 to the progeny of the heterozygous transgenic animals, which included both heterozygous control animals and *wts-1* homozygous mutant animals, on days 1, 2 and 3 after egg laying. In the 1-, 2- and 3-day-old heterozygous control animals, GFP::ACT-5 localized solely to the apical membrane in the intestine when observed 1 hour after heat shock ($n=30$, 8 and 7 for day 1, day 2 and day 3, respectively; Fig. 6Aa). GFP::ACT-5 even remained at the apical region 2 days after the heat shock pulse ($n=40$; Fig. 6Ab). We observed a similar localization pattern of GFP::ACT-5 when 1-day-old mutant animals were observed 1 hour after the heat shock pulse ($n=30$; Fig. 6Ba). By contrast, the

2- and 3-day-old *wts-1* mutant animals had different patterns of ACT-5 localization after heat shock: they showed abnormal localization of GFP::ACT-5 to the basolateral sides and ectopic luminal domains ($n=12$ and 9 for 2- and 3-day-old mutants, respectively; Fig. 6Bc,d). Interestingly enough, GFP::ACT-5 did not label the ectopic luminal domain when 1-day-old *wts-1* mutant animals were given heat shock on day 1 and were observed after 2 days, even though they formed vesicle-like structures ($n=12$; Fig. 6Bb). These data suggest that the localization of newly synthesized GFP::ACT-5 was misregulated in *wts-1* mutant animals at a late time point.

From the phenotype caused by the *wts-1* mutation, it is conceivable that the normal function of WTS-1 is to prevent apical and junctional proteins from being mis-sorted to the ectopic apical or basolateral regions of the membrane. To confirm this, we performed RNAi experiments against candidate genes known to mediate intracellular trafficking (Fig. 7A). RNAi of several genes that are involved in the endocytosis, such as *rme-8*, *cup-4*, *cup-5* and *dnj-25* (Grant and Sato, 2006) did not suppress the *wts-1* mutant phenotype (J.K. and J.L., unpublished). Interestingly, we found that RNAi of exocyst complex genes suppressed the intracellular vesicle-like localization of GFP::ACT-5 in the *wts-1* mutant animals. Although not all genes showed the suppression phenotype, probably due to an incomplete RNA interference effect, RNAi of *sec-5*, *sec-6*, *sec-8*, *sec-10* and *sec-15* significantly suppressed the severe intracellular vesicle-like GFP::ACT-5 localization phenotype in *wts-1* mutant animals (Fig. 7B; see Table S3 in the supplementary material). RNAi of the exocyst complex genes did not affect the apical localization of GFP::ACT-5 in the WT and *wts-1* mutant animals (Fig. 7B; see Fig. S4 and Tables

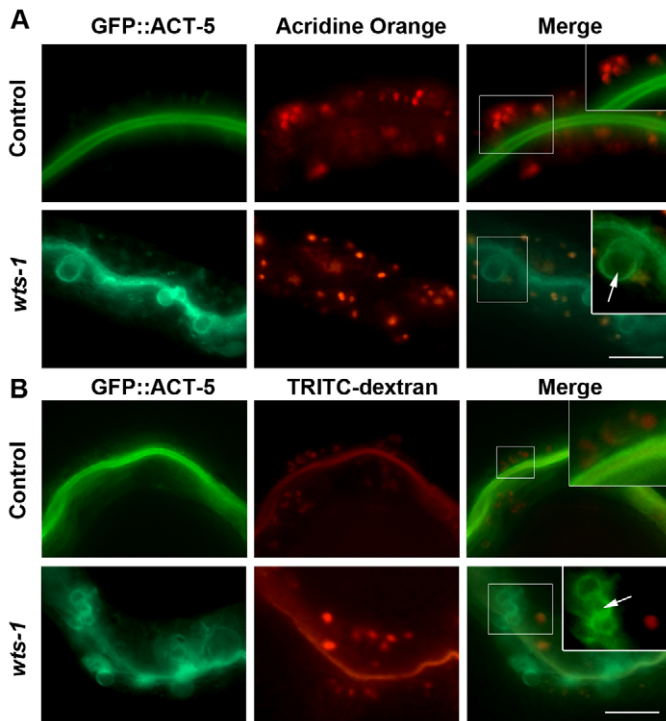


Fig. 5. The vesicle-like structures are not endocytic vesicles.

(A,B) Results of the endocytosis test following feeding of endosomal markers Acridine Orange (AO, A) and TRITC-dextran (B). GFP::ACT-5 (green), and AO or TRITC-dextran (red) in wild-type worms (Control) and *wts-1(ok753)* (*wts-1*) mutant animals. Insets are magnified images of framed areas; arrows indicate either AO- or TRITC-dextran-negative GFP::ACT-5 vesicles in *wts-1* mutant animals. Scale bars: 10 μ m.

S3 and S4 in the supplementary material). These results suggest that exocyst complex genes are required for the mislocalization of apical actin in the *wts-1* mutant animals.

DISCUSSION

The *C. elegans* genome contains genes that encode the homologous proteins of the components of Hpo pathway, *cst-1* and *cst-2* for *hpo*, T10H10.3 for *sav* and *wts-1* for *wts*, suggesting that the Hpo pathway might have evolutionarily conserved roles in *C. elegans*. Although the roles of the Hpo pathway in cell proliferation and apoptosis have already been well characterized, its involvement in cell integrity has not been well studied. Our study now firmly establishes that WTS-1 has additional roles in cell integrity in intestinal cells by regulating the localization of apical actin and junctional proteins. An examination of the intestinal degenerative phenotypes of *wts-1* mutant animals revealed that intestinal apical actin and Ce_AJ components are gradually dispersed to the ectopic apical region.

Although the exact cause of the larval arrest phenotype caused by the *wts-1* mutation is not clear at this point, it is obvious that *wts-1* is essential in the intestine, but not in other tissues that normally express WTS-1, such as the hypodermis. The hypodermis is different from the intestine in its anatomy; whereas the hypodermis is a non-tube epithelium, the intestine is a tube-type epithelium. In fact, our preliminary observations suggest that *wts-1* might have redundant functions with other proteins in the hypodermis (J.K. and J.L., unpublished). These facts suggest that WTS-1 might have distinct functions in different types of epithelial tissues.

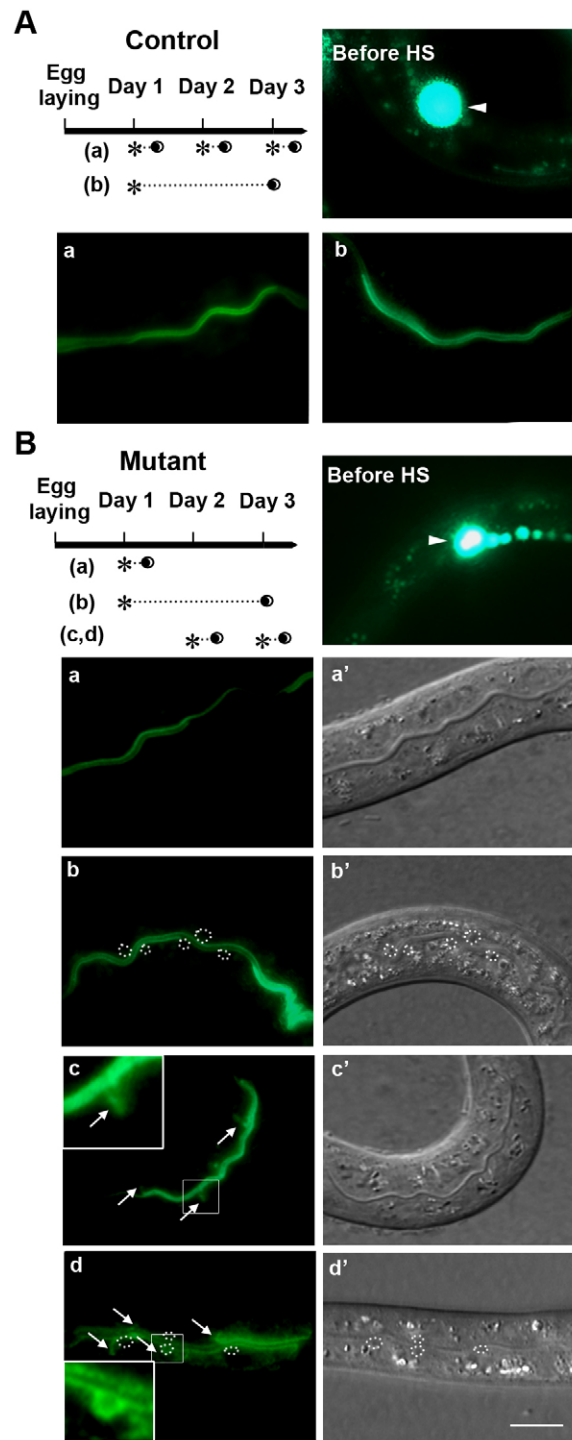


Fig. 6. Newly synthesized GFP::ACT-5 proteins in late *wts-1* mutant animals are mislocalized to ectopical luminal domains. (A,B) Results of the heat-shock-based GFP::ACT-5 pulse-chase experiments. Left upper panels are schematics of heat-shock-based GFP::ACT-5 pulse-chase experiments in control (A) and *wts-1* mutant (B) animals. Lowercase letters indicate images of each experiment. Asterisks indicate the start point of heat shock for 20 minutes at 33°C. Partially filled circles indicate the time point of observation. Control and mutant worms are *wts-1(ok753)/hT2*; Ex[Phsp::gfp::act-5, pRF4] and *wts-1(ok753)*; Ex[Phsp::gfp::act-5, pRF4], respectively. Arrowheads indicate nonspecific GFP::ACT-5 expression in neuronal cells before heat shock. Arrows in B indicate basolaterally localized GFP::ACT-5. Insets are magnified images. Dotted circles indicate ectopic luminal domains. Scale bar: 10 μ m.

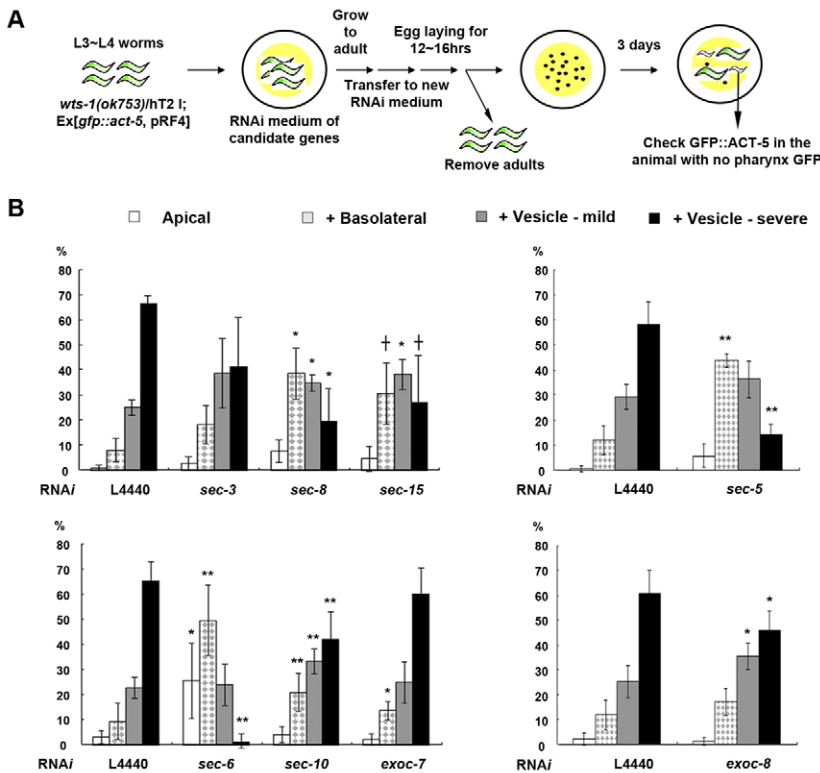


Fig. 7. Exocyst complex is required for the mislocalization of apical actin in *wts-1* mutant animals. (A) Schematic showing the procedure of the RNAi screen assay. *wts-1(ok753)/hT2; Ex[gfp::act-5, pRF4]* worms were used in this assay and *wts-1* mutant animals were recognized by the lack of pharynx GFP signal. (B) Quantification of the results of the RNAi assay for representative exocyst complex genes. 'Apical' indicates apical GFP::ACT-5 localization; '+ Basolateral' indicates apical and basolateral GFP::ACT-5 localization; '+ Vesicle-mild' indicates that there were one to three additional lumen-like structures per intestinal cell; '+ Vesicle-severe' indicates more than three additional lumen-like structures. *, $P < 0.05$; **, $P < 0.01$; †, $P < 0.1$.

The observation that newly hatched *wts-1* mutant larvae did not have severe intestine defects seems to suggest that *wts-1* is not involved in the initial establishment of intestinal apical structure, but is probably involved in its maintenance. However, it is still possible that *wts-1* is involved in the establishment of intestinal apical structure. First, it is possible that any severe phenotype might have been masked by maternal WTS-1 proteins provided by the heterozygous mothers. This possibility seems unlikely, because the intestine-specific rescue line, in which only zygotic expression of WTS-1 in the intestine was restored, was fertile and did not have any defects. The promoter we used for the intestine-specific rescue was from the *opt-2* gene, which is active only after the epithelization of the embryonic intestine tissue (J.K. and J.L., unpublished). If the maternal supply of WTS-1 was essential for the initial establishment of the apical structures, the intestine-specific expression line would exhibit intestine defects. Second, it is possible that *wts-1* is indeed involved in the establishment of intestinal apical structure, but is redundant with other factors. It is known that multiple polarization pathways are involved in cell polarity establishment, thereby creating genetic redundancy, and that the inactivation of any single pathway does not completely destroy cell integrity (Labouesse, 2006; Totong et al., 2007). Therefore, it is possible that a single mutation of *wts-1* might not disrupt cell integrity at the beginning of the establishment of intestinal apical structure. If this is the case, it will be possible to identify genes that act redundantly with *wts-1*.

Lats kinases have been studied for their roles in mitosis and cytokinesis (McPherson et al., 2004; Yang et al., 2004). Consistent with their known functions in mammals, it has been reported that LATS1 localizes to the mitotic apparatus, centrosome and midbody during cell division (Hirota et al., 2000; Yang et al., 2004). LATS2 is also known to localize to the centrosome during the cell cycle (McPherson et al., 2004). Yet other reports have suggested that Lats kinases are localized to subcellular compartments unrelated to

mitosis or cytokinesis. For example, in flies it has been reported that Wts preferentially localizes near the membrane, where it may influence tissue polarity, growth and gene expression (Cho et al., 2006). Cbk1 is also known to localize to sites of polarized growth and regulate bud emergence, growth and maintenance of cell integrity in yeast cells. In addition, many components of the Lats pathway (Mst kinase, Mer, Ex, Mob1 and Yap) localize to the membrane (Boedigheimer et al., 1997; Hergovich et al., 2005; Katagiri et al., 2006; Lallemand et al., 2003; Mohler et al., 1999). Our data clearly show that WTS-1 is localized to the subapical region in the intestine. The subapical membrane in epithelial cells is generally important for polarization because active exocytosis and membrane growth occur at subapical membranes (Mostov et al., 2003; Nelson, 2003). Consistent with the normal function of WTS-1 in inhibiting the mislocalization of intestinal apical actin, knockdown of the exocyst complex proteins, which are known to be important for protein targeting to the basolateral membrane (Grindstaff et al., 1998), suppresses the ectopic localization of apical actin in the *wts-1* mutant animals. These facts strongly suggest that *wts-1* acts as a guardian to ensure that the apical actin and junctional proteins are properly transported and maintained near the plasma membrane to preserve normal lumen structures. Collectively, our data and the data of others strongly suggest the possibility that an evolutionarily conserved function of Lats is to regulate apical protein localization to maintain cell integrity in epithelial cells. It would be of interest to examine whether the regulation of protein localization by *wts-1* is conserved in other species, such as *D. melanogaster* and mammals. In addition, the phenotype associated with the *wts-1* mutation in *C. elegans* is related, but not identical, to the phenotype seen with mutations in *crumbs* and *stardust* in *D. melanogaster*, both of which are crucial elements in the regulation of epithelial cell polarity (Bachmann et al., 2001). It would be of interest to examine the roles of homologs of these genes in the maintenance of cellular polarity in *C. elegans*.

How does WTS-1 regulate the integrity of the intestine? One possible mechanism is by regulating the localization of a subset of proteins through phosphorylation. It is known that PAR-1 phosphorylates BAZ, the PAR-3 homolog in *D. melanogaster*, causing BAZ to bind 14-3-3 and thereby inhibiting the basolateral localization of BAZ (Benton and St Johnston, 2003). aPKC also phosphorylates PAR-1 to regulate the localization of PAR-1 (Hurov et al., 2004). Likewise, *wts-1* might phosphorylate target proteins that regulate cellular integrity. Interestingly, Cbk1 in budding yeasts binds and phosphorylates Sec2, a guanyl-nucleotide exchange factor (GEF), which is involved in polarized growth and secretion in yeast (Kurischko et al., 2008). There are many GEF homologs in *C. elegans*, and it would be of interest to examine whether any of these can be phosphorylated by WTS-1. Another possibility is that Lats kinase might be directly involved in the actin filament assembly. LATS1 in mammals is known to bind the actin-cytoskeleton-associated proteins zyxin and LIMK1 (Hirota et al., 2000; Yang et al., 2004). During mitosis and cytokinesis, LATS1 colocalizes with F-actin. During cytokinesis, LATS1 negatively regulates LIMK1, subsequently affecting cofilin and actin polymerization (Yang et al., 2004). Likewise, it is possible that Lats kinase modulates actin organization at the membrane by regulating the localization or the activity of actin-associated proteins, and mediates the organization of microvilli structure at the apical membrane. Further studies are needed to determine which proteins are primarily responsible for the *wts-1* action in *C. elegans*.

The multiple lumen-like-structure phenotype of the *wts-1* mutant animals is similar to the phenotype observed in human patients with microvillus inclusion disease (MVID). In addition, the fact that these patients die before 20 months of age is analogous to the L1 to L2 larval arrest phenotype of *wts-1* (Ameen and Salas, 2000; Beck et al., 2001). Interestingly, defects in protein trafficking are thought to be the major pathogenic factor underlying MVID. For example, abnormal apical membrane protein trafficking or misregulated endocytosis can lead to MVID (Ameen and Salas, 2000; Sato et al., 2007). Further studies are needed to determine whether the malfunction of Lats kinases and the genes that are involved in protein targeting/sorting are involved in MVID pathogenesis.

Acknowledgements

We thank D. Lim (KAIST, Korea) for his advice on the initiation of this study. We also thank the CGC for strains, Y. Kohara for cDNA constructs, J. Ahringer for RNAi plasmids, K. Nehrke and M. Han for vectors and K. Kemphues for antibodies. This work was supported by a KOSEF grant (R01-2006-000-10623-0), a KRF grant (KRF-2008-005-J00201), a WCU program (305-20080089) and the RCFC, Seoul National University, Seoul, Korea. J.K. was supported by a Seoul Science Fellowship.

Supplementary material

Supplementary material for this article is available at <http://dev.biologists.org/cgi/content/full/136/16/2705/DC1>

References

- Ameen, N. A. and Salas, P. J. (2000). Microvillus inclusion disease: a genetic defect affecting apical membrane protein traffic in intestinal epithelium. *Traffic* **1**, 76-83.
- Bachmann, A., Schneider, M., Theilenberg, E., Grawe, F. and Knust, E. (2001). *Drosophila* Stardust is a partner of Crumbs in the control of epithelial cell polarity. *Nature* **414**, 638-643.
- Beck, N. S., Kang, I. S. and Suh, Y. L. (2001). Protracted diarrhea: results of the five-year survey in a tertiary hospital in Korea. *J. Korean Med. Sci.* **16**, 736-741.
- Benton, R. and St Johnston, D. (2003). *Drosophila* PAR-1 and 14-3-3 inhibit Bazooka/PAR-3 to establish complementary cortical domains in polarized cells. *Cell* **115**, 691-704.
- Bidlingmaier, S., Weiss, E. L., Seidel, C., Drubin, D. G. and Snyder, M. (2001). The Cbk1p pathway is important for polarized cell growth and cell separation in *Saccharomyces cerevisiae*. *Mol. Cell. Biol.* **21**, 2449-2462.
- Boedigheimer, M. J., Nguyen, K. P. and Bryant, P. J. (1997). Expanded functions in the apical cell domain to regulate the growth rate of imaginal discs. *Dev. Genet.* **20**, 103-110.
- Bossinger, O., Klebes, A., Segbert, C., Theres, C. and Knust, E. (2001). Zonula adherens formation in *Caenorhabditis elegans* requires dlg-1, the homologue of the *Drosophila* gene discs large. *Dev. Biol.* **230**, 29-42.
- Bossinger, O., Fukushige, T., Claeys, M., Borgonie, G. and McGhee, J. D. (2004). The apical disposition of the *Caenorhabditis elegans* intestinal terminal web is maintained by LET-413. *Dev. Biol.* **268**, 448-456.
- Branicky, R. and Hekimi, S. (2006). What keeps *C. elegans* regular: the genetics of defecation. *Trends Genet.* **22**, 571-579.
- Cho, E., Feng, Y., Rauskolb, C., Maitra, S., Fehon, R. and Irvine, K. D. (2006). Delineation of a Fat tumor suppressor pathway. *Nat. Genet.* **38**, 1142-1150.
- Costa, M., Raich, W., Agbunag, C., Leung, B., Hardin, J. and Priess, J. R. (1998). A putative catenin-cadherin system mediates morphogenesis of the *Caenorhabditis elegans* embryo. *J. Cell Biol.* **141**, 297-308.
- Cox, E. A. and Hardin, J. (2004). Sticky worms: adhesion complexes in *C. elegans*. *J. Cell Sci.* **117**, 1885-1897.
- Dong, J., Feldmann, G., Huang, J., Wu, S., Zhang, N., Comerford, S. A., Gayyed, M. F., Anders, R. A., Maitra, A. and Pan, D. (2007). Elucidation of a universal size-control mechanism in *Drosophila* and mammals. *Cell* **130**, 1120-1133.
- Emoto, K., Parrish, J. Z., Jan, L. Y. and Jan, Y. N. (2006). The tumour suppressor Hippo acts with the NDR kinases in dendritic tiling and maintenance. *Nature* **443**, 210-213.
- Grant, B., Zhang, Y., Paupard, M. C., Lin, S. X., Hall, D. H. and Hirsh, D. (2001). Evidence that RME-1, a conserved *C. elegans* EH-domain protein, functions in endocytic recycling. *Nat. Cell Biol.* **3**, 573-579.
- Grant, B. D. and Sato, M. (2006). Intracellular trafficking. *WormBook*, doi:10.1895/wormbook.1.77.1
- Grindstaff, K. K., Yeaman, C., Anandasabapathy, N., Hsu, S. C., Rodriguez-Boulan, E., Scheller, R. H. and Nelson, W. J. (1998). Sec6/8 complex is recruited to cell-cell contacts and specifies transport vesicle delivery to the basal-lateral membrane in epithelial cells. *Cell* **93**, 731-740.
- Harvey, K. and Tapon, N. (2007). The Salvador-Warts-Hippo pathway-an emerging tumour-suppressor network. *Nat. Rev. Cancer* **7**, 182-191.
- Hedgecock, E. M. and White, J. G. (1985). Polyploid tissues in the nematode *Caenorhabditis elegans*. *Dev. Biol.* **107**, 128-133.
- Hergovich, A., Bichsel, S. J. and Hemmings, B. A. (2005). Human NDR kinases are rapidly activated by MOB proteins through recruitment to the plasma membrane and phosphorylation. *Mol. Cell. Biol.* **25**, 8259-8272.
- Hergovich, A., Stegert, M. R., Schmitz, D. and Hemmings, B. A. (2006). NDR kinases regulate essential cell processes from yeast to humans. *Nat. Rev. Mol. Cell Biol.* **7**, 253-264.
- Hirota, T., Morisaki, T., Nishiyama, Y., Marumoto, T., Tada, K., Hara, T., Masuko, N., Inagaki, M., Hatakeyama, K. and Saya, H. (2000). Zyxin, a regulator of actin filament assembly, targets the mitotic apparatus by interacting with h-warts/LATS1 tumor suppressor. *J. Cell Biol.* **149**, 1073-1086.
- Hurov, J. B., Watkins, J. L. and Pivnicka-Worms, H. (2004). Atypical PKC phosphorylates PAR-1 kinases to regulate localization and activity. *Curr. Biol.* **14**, 736-741.
- Jiang, Z., Li, X., Hu, J., Zhou, W., Jiang, Y., Li, G. and Lu, D. (2006). Promoter hypermethylation-mediated down-regulation of LATS1 and LATS2 in human astrocytoma. *Neurosci. Res.* **56**, 450-458.
- Justice, R. W., Zilian, O., Woods, D. F., Noll, M. and Bryant, P. J. (1995). The *Drosophila* tumor suppressor gene warts encodes a homolog of human myotonic dystrophy kinase and is required for the control of cell shape and proliferation. *Genes Dev.* **9**, 534-546.
- Katagiri, K., Imamura, M. and Kinashi, T. (2006). Spatiotemporal regulation of the kinase Mst1 by binding protein RAP1 is critical for lymphocyte polarity and adhesion. *Nat. Immunol.* **7**, 919-928.
- Ko, K. M., Lee, W., Yu, J. R. and Ahnn, J. (2007). PYP-1, inorganic pyrophosphatase, is required for larval development and intestinal function in *C. elegans*. *FEBS Lett.* **581**, 5445-5453.
- Kurischko, C., Kuravi, V. K., Wannissorn, N., Nazarov, P. A., Husain, M., Zhang, C., Shokat, K. M., McCaffery, J. M. and Luca, F. C. (2008). The yeast LATS/Ndr kinase Cbk1 regulates growth via Golgi-dependent glycosylation and secretion. *Mol. Biol. Cell* **19**, 5559-5578.
- Labouesse, M. (2006). Epithelial junctions and attachments. *WormBook*, doi:10.1895/wormbook.1.56
- Lallemant, D., Curto, M., Saotome, I., Giovannini, M. and McClatchey, A. I. (2003). NF2 deficiency promotes tumorigenesis and metastasis by destabilizing adherens junctions. *Genes Dev.* **17**, 1090-1100.
- Leung, B., Hermann, G. J. and Priess, J. R. (1999). Organogenesis of the *Caenorhabditis elegans* intestine. *Dev. Biol.* **216**, 114-134.
- Liu, D. W. and Thomas, J. H. (1994). Regulation of a periodic motor program in *C. elegans*. *J. Neurosci.* **14**, 1953-1962.
- MacQueen, A. J., Baggett, J. J., Perumov, N., Bauer, R. A., Januszewski, T., Schriefer, L. and Waddle, J. A. (2005). ACT-5 is an essential *Caenorhabditis*

- elegans actin required for intestinal microvilli formation. *Mol. Biol. Cell* **16**, 3247-3259.
- McPherson, J. P., Tambllyn, L., Elia, A., Migon, E., Shehabeldin, A., Matysiak-Zablocki, E., Lemmers, B., Salmena, L., Hakem, A., Fish, J. et al.** (2004). Lats2/Kpm is required for embryonic development, proliferation control and genomic integrity. *EMBO J.* **23**, 3677-3688.
- Meignin, C., Alvarez-Garcia, I., Davis, I. and Palacios, I. M.** (2007). The Salvador-Warts-Hippo pathway is required for epithelial proliferation and axis specification in *Drosophila*. *Curr. Biol.* **17**, 1871-1878.
- Mohler, P. J., Kreda, S. M., Boucher, R. C., Sudol, M., Stutts, M. J. and Milgram, S. L.** (1999). Yes-associated protein 65 localizes p62(c-Yes) to the apical compartment of airway epithelia by association with EBP50. *J. Cell Biol.* **147**, 879-890.
- Mostov, K., Su, T. and ter Beest, M.** (2003). Polarized epithelial membrane traffic: conservation and plasticity. *Nat. Cell Biol.* **5**, 287-293.
- Nehrke, K.** (2003). A reduction in intestinal cell pH due to loss of the *Caenorhabditis elegans* Na⁺/H⁺ exchanger NHX-2 increases life span. *J. Biol. Chem.* **278**, 44657-44666.
- Nelson, W. J.** (2003). Adaptation of core mechanisms to generate cell polarity. *Nature* **422**, 766-774.
- Oka, T., Toyomura, T., Honjo, K., Wada, Y. and Futai, M.** (2001). Four subunit a isoforms of *Caenorhabditis elegans* vacuolar H⁺-ATPase. Cell-specific expression during development. *J. Biol. Chem.* **276**, 33079-33085.
- Pfeiffer, J., Johnson, D. and Nehrke, K.** (2008). Oscillatory transepithelial H⁺ flux regulates a rhythmic behavior in *C. elegans*. *Curr. Biol.* **18**, 297-302.
- Polesello, C. and Tapon, N.** (2007). Salvador-Warts-Hippo signaling promotes *Drosophila* posterior follicle cell maturation downstream of notch. *Curr. Biol.* **17**, 1864-1870.
- Portereiko, M. F. and Mango, S. E.** (2001). Early morphogenesis of the *Caenorhabditis elegans* pharynx. *Dev. Biol.* **233**, 482-494.
- Sato, T., Mushiaki, S., Kato, Y., Sato, K., Sato, M., Takeda, N., Ozono, K., Miki, K., Kubo, Y., Tsuji, A. et al.** (2007). The Rab8 GTPase regulates apical protein localization in intestinal cells. *Nature* **448**, 366-369.
- Saucedo, L. J. and Edgar, B. A.** (2007). Filling out the Hippo pathway. *Nat. Rev. Mol. Cell Biol.* **8**, 613-621.
- Starich, T. A., Miller, A., Nguyen, R. L., Hall, D. H. and Shaw, J. E.** (2003). The *Caenorhabditis elegans* innexin INX-3 is localized to gap junctions and is essential for embryonic development. *Dev. Biol.* **256**, 403-417.
- St John, M. A., Tao, W., Fei, X., Fukumoto, R., Carcangiu, M. L., Brownstein, D. G., Parlow, A. F., McGrath, J. and Xu, T.** (1999). Mice deficient of Lats1 develop soft-tissue sarcomas, ovarian tumours and pituitary dysfunction. *Nat. Genet.* **21**, 182-186.
- Takahashi, Y., Miyoshi, Y., Takahata, C., Irahara, N., Taguchi, T., Tamaki, Y. and Noguchi, S.** (2005). Down-regulation of LATS1 and LATS2 mRNA expression by promoter hypermethylation and its association with biologically aggressive phenotype in human breast cancers. *Clin. Cancer Res.* **11**, 1380-1385.
- Totong, R., Achilleos, A. and Nance, J.** (2007). PAR-6 is required for junction formation but not apicobasal polarization in *C. elegans* embryonic epithelial cells. *Development* **134**, 1259-1268.
- Verde, F., Wiley, D. J. and Nurse, P.** (1998). Fission yeast orb6, a ser/thr protein kinase related to mammalian rho kinase and myotonic dystrophy kinase, is required for maintenance of cell polarity and coordinates cell morphogenesis with the cell cycle. *Proc. Natl. Acad. Sci. USA* **95**, 7526-7531.
- Xu, T., Wang, W., Zhang, S., Stewart, R. A. and Yu, W.** (1995). Identifying tumor suppressors in genetic mosaics: the *Drosophila* lats gene encodes a putative protein kinase. *Development* **121**, 1053-1063.
- Yang, X., Yu, K., Hao, Y., Li, D. M., Stewart, R., Insogna, K. L. and Xu, T.** (2004). LATS1 tumour suppressor affects cytokinesis by inhibiting LIMK1. *Nat. Cell Biol.* **6**, 609-617.
- Yu, J., Poulton, J., Huang, Y. C. and Deng, W. M.** (2008). The hippo pathway promotes Notch signaling in regulation of cell differentiation, proliferation, and oocyte polarity. *PLoS ONE* **3**, e1761.
- Zhao, B., Wei, X., Li, W., Udan, R. S., Yang, Q., Kim, J., Xie, J., Ikenoue, T., Yu, J., Li, L. et al.** (2007). Inactivation of YAP oncoprotein by the Hippo pathway is involved in cell contact inhibition and tissue growth control. *Genes Dev.* **21**, 2747-2761.

Table S1. *wts-1* phenotype of *wts-1* mutant and *wts-1* RNAi animals**A. *wts-1* phenotype in control and *wts-1(ok753)* mutant animals**

Genotype		Control	Mutant
		<i>dpy-5(e61) daf-16(m26) unc-75(e950)</i>	<i>wts-1(ok753)</i>
Phenotype			
Emb		1 (1%)	31 (8%)
Lva		0 (0%)	332 (92%)
<i>n</i>		193	363

B. *wts-1* phenotype in RNAi animals

Genotype		Control		<i>wts-1</i>	
		<i>N2</i>	<i>rrf-3</i>	<i>N2</i>	<i>rrf-3</i>
Phenotype					
Emb		0 (0%)	11 (6%)	0 (0%)	7 (6%)
Lva		0 (0%)	2 (1%)	24 (21%)	116 (92%)
<i>n</i>		103	196	112	126

To calculate the embryonic and larval lethality of *wts-1*, we checked the phenotype in *wts-1* mutant animals of the progeny of *wts-1(ok753)/dpy-5(e61) daf-16(m26) unc-75(e950)*. Homozygotes of *dpy-5(e61) daf-16(m26) unc-75(e950)* were used as a control.

Emb, Embryonic lethality; Lva, L1 larval arrest.

Table S2. Protein markers in control and *wts-1* mutant worms

	Control (heterozygotes)			<i>wts-1(ok753)</i> homozygotes		
A. GFP::ACT-5 localization in control and <i>wts-1</i> mutant worms						
Time	Day 1	Day 2	Day 3	Day 1	Day 2	Day 3
Apical only	150 (96±2%)	157 (97±1%)	137 (98±2%)	42 (38±12%)	4 (5±2%)	0 (0±0%)
Apical + basolateral	5 (3±2%)	3 (2±2%)	1 (1±2%)	65 (59±10%)	28 (38±9%)	1 (1±2%)
Apical + basolateral + vesicle	2 (1±1%)	2 (1±2%)	1 (1±1%)	3 (3±2%)	41 (56±10%)	67 (99±2%)
<i>n</i>	157	162	139	110	73	68
B. Intestinal DLG-1::GFP localization in control and <i>wts-1</i> mutant worms						
Time	Day 1	Day 3	Day 1	Day 3		
Normal	77 (99±2%)	70 (99±4%)	26 (84±12%)	20 (29±21%)		
Abnormal	1 (1±2%)	1 (1±4%)	5 (16±12%)	49(71±21%)		
<i>n</i>	78	71	31	69		
C. HMP-1::GFP localization in control and <i>wts-1</i> mutant worms						
Time	Day 1	Day 3	Day 1	Day 3		
Normal	4 (100±0%)	42 (100±0%)	4 (100±0%)	4 (13±3%)		
Abnormal	0 (0±0%)	0 (0±0%)	0 (100±0%)	31 (86±3%)		
<i>n</i>	4	42	4	35		
D. VHA-6::GFP localization in control and <i>wts-1</i> mutant worms						
Time	Day 1	Day 3	Day 1	Day 3		
Normal	101	62	47	63		
+ Vesicle	0	0	1	3		
<i>n</i>	101	62	48	66		
E. OPT-2::GFP localization in control and <i>wts-1</i> mutant worms						
Time	Day 1	Day 3	Day 1	Day 3		
Normal	70	61	20	14		
+ Basolateral	0	0	0	10		
<i>n</i>	70	61	20	24		
F. NHX-7::GFP localization in control and <i>wts-1</i> mutant worms						
Time	Day 1	Day 1	Day 3			
Apical	0	0	0			
Basolateral	61	31	12			
<i>n</i>	61	31	12			
G. INX-3::GFP localization in control and <i>wts-1</i> mutant worms						
Time	Day 1	Day 1	Day 3			
Apical	0	0	0			
Basolateral	>50	>50	23			
<i>n</i>	>50	>50	23			

Table S3. Summary of exocyst complex RNAi in the *wts-1* mutant

	L4440	<i>sec-3</i>	<i>sec-5</i>	<i>sec-6</i>	<i>sec-8</i>	<i>sec-10</i>	<i>sec-15</i>	<i>exoc-7</i>	<i>exoc-8</i>
Apical only	7 (2%)	4 (3%)	16 (7%)	24 (22%)	11 (7%)	8 (4%)	3 (4%)	5 (2%)	3 (2%)
Apical + basolateral	40 (10%)	24 (19%)	103 (43%)	53 (50%)	59 (37%)	43 (20%)	25 (29%)	25 (13%)	37 (17%)
Apical + basolateral + vesicle – mild	103 (25%)	47 (38%)	88 (37%)	28 (26%)	56 (35%)	72 (33%)	32 (37%)	48 (25%)	76 (35%)
Apical + basolateral + vesicle – severe	266 (63%)	48 (39%)	33 (14%)	2 (2%)	34 (21%)	95 (43%)	26 (30%)	117 (60%)	100 (46%)
<i>n</i>	416	123	240	107	160	218	86	195	216

Table S4. Summary of exocyst complex RNAi in N2 wild-type animals

	L4440	<i>sec-3</i>	<i>sec-5</i>	<i>sec-6</i>	<i>sec-8</i>	<i>sec-10</i>	<i>sec-15</i>	<i>exoc-7</i>	<i>exoc-8</i>
Apical only	121 (97%)	111 (97%)	127 (96%)	93 (94%)	116 (98%)	130 (97%)	141 (98%)	127 (99%)	102 (97%)
Apical + basolateral	2 (2%)	2 (2%)	2 (2%)	2 (2%)	1 (1%)	2 (2%)	3 (2%)	1 (1%)	2 (2%)
Apical + basolateral + vesicle	2 (2%)	2 (2%)	3 (2%)	3 (4%)	2 (1%)	1 (1%)	1 (1%)	0 (0%)	1 (1%)
<i>n</i>	125	115	132	98	119	133	145	128	105